Cerebral Cortex April 2013;23:751–762
doi:10.1093/cercor/bhs092
Advance Access publication April 11, 2012

FEATURE ARTICLE
Chronic In Vivo Imaging Shows No Evidence of Dendritic Plasticity or Functional Remapping in the Contralesional Cortex after Stroke

David G. Johnston[1,2], Marie Denizet[1,4], Ricardo Mostany[1] and Carlos Portera-Cailliau[1,3]

[1]Department of Neurology, [2]Neuroscience Interdepartmental Program and [3]Department of Neurobiology, David Geffen School of Medicine at UCLA, Los Angeles, CA 90095
[4]Current address: École Normale Supérieure, Paris, 75005, France

Address correspondence to Dr Carlos Portera-Cailliau, Departments of Neurology and Neurobiology, David Geffen School of Medicine at UCLA, Reed Neurological Research Center, Room A-145, 710 Westwood Plaza, Los Angeles, CA 90095, USA. Email: cpcailliau@mednet.ucla.edu.

Most stroke survivors exhibit a partial recovery from their deficits. This presumably occurs because of remapping of lost capabilities to functionally related brain areas. Functional brain imaging studies suggest that remapping in the contralateral uninjured cortex might represent a transient stage of compensatory plasticity. Some postmortem studies have also shown that cortical lesions, including stroke, can trigger dendritic plasticity in the contralateral hemisphere, but the data are controversial. We used longitudinal in vivo two-photon microscopy in the contralateral homotopic cortex to record changes in dendritic spines of layer 5 pyramidal neurons in green fluorescent protein mice. We could not detect de novo growth of dendrites or changes in the density or turnover of spines for up to 4 weeks after stroke. We also used intrinsic optical signal imaging to investigate whether the forepaw (FP) sensory representation is remapped to the spared homotopic cortex after stroke. Stimulation of the contralateral FP reliably produced strong intrinsic signals in the spared hemisphere, but we could never detect a signal with ipsilateral FP stimulation after stroke. This lack of contralateral plasticity at the level of apical dendrites of layer 5 pyramidal neurons and FP sensory maps suggests that the contralesional cortex may not contribute to functional recovery after stroke and that, at least in mice, the peri-infarct cortex plays the dominant role in postischemic plasticity.

Keywords: intrinsic optical signal imaging, ischemia, middle cerebral artery occlusion, rose Bengal, 2-photon

Introduction

Although mortality from stroke has decreased through advances in critical care medicine, survivors are often left with profound lifetime sequelae, and stroke remains the leading cause of adult onset disability in the United States (Lloyd-Jones et al. 2009). This has led some experts to suggest that a better strategy for treatment of stroke is to focus on brain repair and rehabilitation in order to improve functional recovery (Grotta et al. 2008). The speech, sensory, and motor deficits after stroke are a direct result of neuronal death in areas of brain infarction. Remarkably, many patients partially recover from these deficits over days to months (Twitchell 1951; Skilbeck et al. 1983), and the potential for recovery appears to be far greater in children, perhaps because their developing brain has a greater potential for neuronal plasticity (Johnston 2009; Kim et al. 2009).

Functional recovery after stroke is presumably mediated by compensatory remapping of lost capabilities to functionally related brain regions in both hemispheres that were performing similar but were spared by the infarct (Glees and Cole 1950; Chollet et al. 1991; Cao et al. 1998; Dijkhuizen et al. 2001; Schaechter and Perdue 2008). The peri-infarct cortex, which suffers slight decreases in blood flow but little if any neuronal damage (Witte et al. 2000), exhibits both functional and structural forms of plasticity, particularly at level of dendrites (reviewed by Murphy and Corbett 2009; Zhang and Chopp 2009). But it is conceivable that such remodeling in peri-infarct cortex could be a manifestation of deafferentation or could be triggered by mild ischemia, inflammation, or pathological changes in the nearby infarct. As such, these plastic changes might represent a purely maladaptive response that could eventually lead to circuit dysfunction. Moreover, it is not clear that changes in dendrites in peri-infarct cortex can fully account for the earliest phase of behavioral improvement that occurs within days after stroke in mice (Brown et al. 2009; Mostany et al. 2010).

Instead, the contralateral hemisphere, which is unaffected by the stroke, might be better equipped to support structural and functional plasticity, even though no mechanism has yet been established for how this might occur. Functional brain imaging studies in humans have suggested the existence of two sequential phases of remapping (Marshall et al. 2000; Dijkhuizen et al. 2001). Lost functions would initially be shifted to the spared hemisphere and later, as inflammation subsides and blood flow improves, those functions are taken over by the peri-infarct cortex. But long-term functional recovery is inversely correlated with how long the impaired function is remapped to the contralateral cortex (Rossini et al. 2003), suggesting it may not be ideal for the spared hemisphere to permanently play the compensatory role.

The structural rewiring underlying such functional remapping to contralateral cortex is also not fully understood. Initial postmortem Golgi studies in fixed tissue have documented that cortical lesions (including stroke) trigger extensive dendritic growth in the contralateral hemisphere (Jones and Schallert 1992, 1994), but subsequent studies could not replicate those results (Forgie et al. 1996; Prusky and Whishaw 1996; Biernaskie et al. 2004; Gibb et al. 2010). These discrepancies, which could arise due to sampling biases from using the Golgi method, must be resolved for us to understand the role of dendritic plasticity after stroke.

In summary, there are several unanswered questions and controversies regarding structural and functional neuronal plasticity after stroke that could be resolved with longitudinal in vivo imaging: Does the contralateral cortex exhibit structural dendritic plasticity or functional remapping after stroke? If so, what is the timing of functional remapping and dendritic plasticity in the spared hemisphere relative to the peri-infarct

cortex? Is plasticity after stroke developmentally regulated, such that younger animals are more likely to exhibit plasticity in the contralateral cortex? We examined these issues in vivo with chronic intrinsic optical signal (IOS) imaging and high-resolution two-photon imaging of dendritic spines of layer (L) 5 pyramidal neurons before and up to 4 weeks after stroke. We found no evidence of dendritic plasticity or functional remapping in the contralesional cortex after stroke induced by either Rose Bengal photothrombosis (RBPT) or permanent unilateral middle cerebral artery occlusion (MCAO).

Materials and Methods

All materials were purchased from Sigma-Aldrich (St Louis, MO) unless otherwise stated.

Animals

We used adult (2–6 months of age) and juvenile (<3 weeks of age) male and female C57BL/6J mice. For in vivo imaging of dendritic structure, we used the GFP-M line of transgenic mice (green fluorescent protein [GFP] expression under the Thy-1 promoter; Feng et al. 2000). All the procedures described in this study were approved by the University of California Chancellor's Animal Research Committee.

Cranial Window Surgery for In Vivo Two-photon Imaging

Chronic glass-covered cranial windows were implanted as previously described (Mostany and Portera-Cailliau 2008; Holtmaat et al. 2009). Mice were anesthetized with isoflurane (1.5% via nose cone) and placed on a stereotaxic frame over a warm water recirculating blanket. Dexamethasone (0.2 mg/kg; Baxter Healthcare Corp., Deerfield, IL) and carprofen (5 mg/kg; Pfizer Inc., New York, NY) were administered subcutaneously to reduce brain edema and local tissue inflammation. A 2.5 mm diameter craniotomy was performed under sterile conditions with a pneumatic dental drill, 3 mm lateral to the midline, and 1.95 mm caudal to Bregma. A sterile 3-mm glass cover slip was gently laid over the dura mater (without using agarose) and glued to the skull with cyanoacrylate-based glue. Dental acrylic was then applied throughout the skull surface and the edges of the cover slip. A titanium bar (0.125 × 0.375 × 0.05 inch) was embedded in the dental acrylic and later used to secure the mouse on to the stage of the microscope for imaging. Cranial windows were implanted at least 3 weeks prior to imaging dendritic spines because transient upregulation of astrocytic and microglial markers has ended by then and because we have shown that control mice have stable spine dynamics within a few days after window implantation (Holtmaat et al. 2009).

Distal MCAO Stroke

Unilateral distal MCAO was performed immediately after the third imaging time point (i.e., last time point for basal conditions; Fig. 1), as previously described (Tamura et al. 1981) with some modifications (Mostany et al. 2010). Mice were anesthetized with isoflurane and placed on a stereotaxic frame over a water recirculating blanket with the head tilted at a 45° angle. The skin between the eye and ear was incised and gently retracted, together with the temporalis muscle. The MCA was identified through the translucent squamosal bone (~0.8 mm rostral to the anterior junction of the zygomatic and squamosal bones), and a tiny (0.7 mm in diameter) craniotomy was performed using a dental drill, ~0.5 mm ventral to the temporal ridge. Next, the MCA was cauterized with the tip of a small forgery iron and transected with a 21G syringe needle. The craniotomy was then covered with a small piece of Gelfoam (Pfizer Inc.). The temporalis muscle and skin were then glued with Vetbond (3M Animal Care Products, St Paul, MN) to the temporal ridge and the acrylic cement of the headset, respectively.

RBPT Stroke

Ischemic infarcts were targeted to the forelimb region of S1 (S1FL) using RBPT as previously described (Watson et al. 1985; Winship and Murphy 2008). Rather than using standard coordinates from a mouse brain Atlas, we used IOS (see below) to record the location of the forepaw (FP) sensory representation in order to target strokes to that area. Mice were anesthetized with isoflurane and placed on a stereotaxic frame. After a midline incision, the scalp over S1 was retracted, and the periosteum gently scraped off with a scalpel blade and cleaned with sterile saline. A Rose Bengal solution (0.4 mL, 1% w/v, 133 mg/kg) was injected intraperitoneally (i.p.), followed immediately by illumination. White light was delivered directly onto the skull surface for 18–19 min using a halogen light source (KL 1500 LCD; Schott North America) coupled to a fiber-optic bundle (aperture 2.75 mm). We performed several calibration experiments to characterize and optimize the RBPT procedure and to produce consistent infarcts in every animal. After illumination, the scalp was sutured and, just as with the other surgeries, the mouse transferred to a warm (37 °C) recovery chamber before being returned to its home cage.

High-Resolution Two-photon Imaging

All imaging was done with a custom-built two-channel two-photon microscope, using a Ti:Sapphire laser (Chameleon Ultra II; Coherent Inc., Santa Clara, CA) tuned to 910 nm, a 40 × 0.8 NA water immersion objective (Olympus, Tokyo, Japan), photomultiplier tubes (Hamamatsu, Japan), and ScanImage software (Pologruto et al. 2003) written in MATLAB (MathWorks, Natick, MA). Imaging of apical dendritic tufts of L5 pyramidal neurons (within 150 μm below the dura) expressing GFP was performed every 4 days (to match previous imaging protocols investigating spine plasticity after input deprivation and stroke; Holtmaat et al. 2006; Mostany et al. 2010) for 36 days (from day –8 to day +28 after MCAO; Fig. 1). Low-magnification image stacks of sparsely labeled L5 neurons were collected (512 × 512 pixels, 0.72 μm/pixel, 5 μm z steps) down to the soma to confirm the identity and dendritic arborization pattern of the cells imaged. High-magnification images (512 × 512 pixels, 0.152 μm/pixel, 1.5 μm apart) were obtained for the analysis of dendritic spines. Regions of interest (ROIs) containing long dendritic segments (average length 53.6 μm) were selected at random for chronic imaging throughout the window. All dendritic protrusions were scored, including those projecting along the z-axis, as long as they protruded >0.5 μm from the shaft. The same dendritic ROIs were located every imaging session using the unique superficial vasculature pattern on the surface of the brain as a reference (Holtmaat et al. 2009). Turnover ratio was defined as (fraction gained + fraction lost)/(2 × total spines). For measurements of dendritic tip length, we aligned the dendritic segments using persistent spines as fiducial points and analyzed, in ImageJ, the lengths of dendritic tips twice before the MCAO (at –4 days and at day 0) and again at +4, +8, +16, +20, +24, and +28 days after MCAO. All imaged tips were in L1, and we focused on dendrites that coursed parallel to the imaging plane.

IOS Imaging

IOS imaging was performed either through the skull covered with a thin layer of dental cement (Fig. 4) or through standard cranial windows (Fig. 5). For the former, we performed a midline scalp incision to expose the skull over S1. The periosteum was gently scraped off, and a thin transparent layer of dental acrylic was then applied to the exposed skull up to the wound margins. Mapping of the receptive field for ipsilateral and contralateral stimulation of the FP was done in the cortex contralateral to the infarct 1–3 days before (PRE) and again at several time points after RBPT or unilateral permanent distal MCAO stroke (+1, +3, +5, +7, +14, and +21 days for adult mice and +1, +3, +7, and +14 days for juvenile mice). For IOS imaging, mice were lightly anesthetized with 0.5–0.75% isoflurane and a single injection of chlorprothixene (6 mg/kg i.p.). In juvenile mice, we implanted cranial windows at P17–P20 and began baseline IOS imaging within 2 days and at the same time points before and after MCAO (as above). As a control, to document that we can see remapping in peri-infarct cortex with IOS through the skull, we also performed IOS imaging after contralateral stimulation of a bundle of 4 whiskers (C2-C3 and D2-D3; WS) and the FP, before and at +5, +13, and +24–28 days after unilateral permanent distal MCAO (not shown). The cortical surface was illuminated by green (535 nm) and red (630 nm) sets of light-emitting diodes (LEDs)

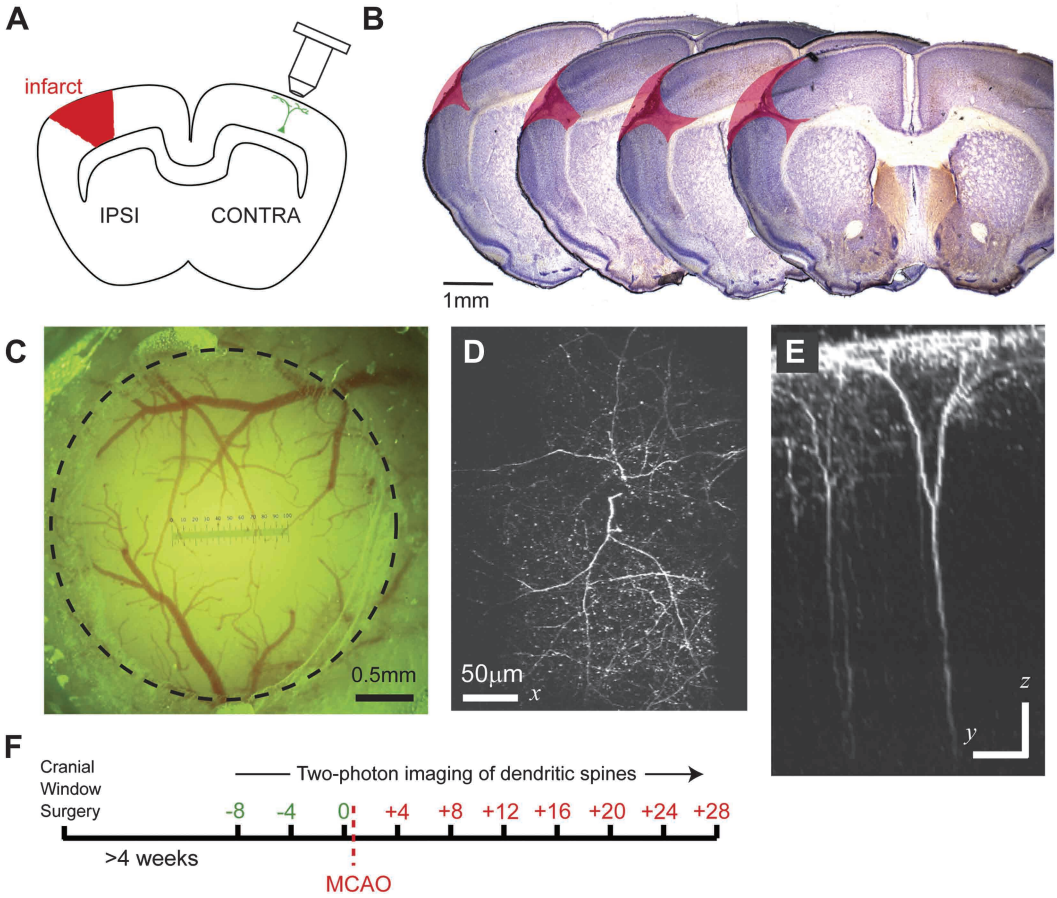

Figure 1. Experimental design and typical MCA stroke. (*A*) Location of cranial window for in vivo imaging area (green neuron) in relation to the location of the infarct (red shaded area). (*B*) Four coronal sections stained with cresyl violet from a mouse in this study, showing the location and size of a representative infarct after MCAO (the red shaded area represents the portions of cortex that was missing when the mouse was perfused at +32 days). (*C*) Sample optical window used for in vivo two-photon imaging. The black dashed circle outlines the window perimeter. Scale bar is 0.5 mm. (*D* and *E*) Representative top view (*D*) and side view (*E*) of an L5 pyramidal neuron expressing GFP in the thy1 GFP-M mouse line at a baseline imaging session before the MCAO. Maximum intensity projection of a stack of 115 images, 5 μm apart (scale bar = 100 μm). (*F*) Experimental timeline for in vivo two-photon imaging experiments.

mounted around a "front-to-front" tandem arrangement of objective lenses (135 and 50 mm focal lengths). The green LEDs were used to visualize the superficial vasculature, and the red LEDs were used for IOS imaging. The microscope was focused to 200–350 μm below the cortical surface, depending on the age of the mouse (deeper for adult mice). Imaging was performed at 30 frames per second using a fast camera (Pantera 1M60; Dalsa), frame grabber (64 Xcelera-CL PX4; Dalsa), and custom routines written in MATLAB. Each session consisted of 30 trials, taken 20 s apart, of mechanical stimulation for 1.5 s (at 10 Hz for whiskers and 100 Hz for FP) using a glass microelectrode (blunt tip for FP) coupled to a piezo bender actuator (Physik Instrumente). Frames 0.9 s before onset of stimulation (baseline) and 1.5 s after stimulation (response) were collected. Frames were binned 3 times temporally and 2 × 2 spatially. Stimulated cortical areas were identified by dividing the response signal by the averaged baseline signal (DR/R) for every trial and then summing all trials. Response maps were then thresholded at 62.5% of maximum response to get the responsive cortical areas for WS and FP stimulation. To determine the strength of the IOS signal map, we calculated a ratio of the average pixel intensity within the map to an equal sized area outside of the map. If a map was not clearly visible when the ipsilateral paw was stimulated, we approximated the presumed area of activity based on the contralateral map and then calculated the ratio. This approach assumes that IOS maps resulting from stimulation of the ipsilateral (affected) FP would be in the exact same region of cortex as those resulting from contralateral FP. We think this is a safe assumption because the idea of remapping to the contralesional cortex makes most sense if it involves neurons that serve the same function but for the opposite hemisphere, so it should follow the same somatotopy. When remapping to the contralateral cortex was previously reported in humans after stroke, the regions involved were the mirror image of the ones in the affected hemisphere (Cao et al. 1998). Moreover, in functional imaging studies that recorded the spread of stimulus-evoked activity from the contralateral to the ipsilateral hemisphere, the same areas were activated in both hemispheres (Mohajerani et al. 2011; Lim et al. 2012).

Statistics

To avoid having to make assumptions required by traditional parametric statistical methods (e.g., normally distributed data), we used resampling methods, including bootstrap versions of one-way and two-way analysis of variance (ANOVA) with repeated measures and linear regression. To perform a one-way ANOVA with repeated measures, we used the ratio of between-group over within-group variability as the test statistic, not as sums of squares as in a traditional *F*-test but as sums of absolute values of the distances from the grand/group means. This ratio was calculated as $(F = \Sigma_{j=1 \ldots m}|(\text{mean } X_j - \text{grand mean})|/\Sigma_{i=1 \ldots n;\ j=1 \ldots m}|X_{ij} - \text{mean } X_j|)$ where m = number of imaging time points, n = number of cells, i = the cell number, and j = the column number. For two-way ANOVA with repeated measures, we performed 3 analyses for the factors (time, experimental treatment, and interaction between factors) as described above. Individual test statistics were calculated for each analysis: time, experimental group, and interaction effect.

To determine statistical significance, data sets were compared against the null hypothesis of no difference between groups. Data sets were resampled with replacement to create new data sets. We then

calculated a new test statistic for the resampled data set. This process was repeated 10 000 times to create a distribution of possible test statistics. The actual test statistic was then compared against this distribution. A two-tailed method was used unless otherwise stated, meaning that statistical significance was determined if the actual test statistic was found in the bottom 2.5 or above the 97.5 percentile of the test statistics from the 10 000 resampled distributions.

For IOS experiments, we used a modified form of linear regression. For this "intercept test," we calculated a distribution of y-intercepts under the null hypothesis to determine if 2 groups had significantly different distributions of y-intercepts. The mean was calculated for each x value and then plotted, and a regression line was then generated using the formula: $y = mx + b$, where m equals the slope of the line and "b" equals the intercept on the y-axis. We chose to use y-intercepts as our test statistic because we found that all of our groups of IOS data had similar slopes, and therefore, differences might be masked if we compared the entire regression since b was the only factor that differed between groups. The data were then bootstrapped 10 000 times to generate a distribution of resampled y-intercepts. Two groups were said to be significantly different if their 95% confidence intervals did not overlap. Significance was set at $P < 0.05$. Error bars in figures are the standard error of the mean. Statistical power calculations indicated that we had sufficient power to detect a 15% difference in spine density, which is a conservative estimate considering that previous labs have reported ~20% differences in spine density before and after stroke in peri-infarct cortex (Brown et al. 2007; Mostany et al. 2010). In terms of the FP stimulation data, we had enough sensitivity to detect a 30% and 35% difference in map size and signal intensity, respectively.

Results

Absence of Dendritic Plasticity in the Contralateral Cortex after Stroke

We and others have used chronic high-resolution in vivo two-photon microscopy to show that dendritic spine remodeling in peri-infarct cortex may contribute to brain repair and functional recovery after stroke (Brown et al. 2007, 2009; Mostany et al. 2010). To investigate whether dendritic spine plasticity also occurs in the contralateral homotopic cortex after stroke, we used the same approach to image GFP-expressing pyramidal neurons through a cranial window before and after permanent unilateral distal MCAO. We chose the same MCAO model of stroke (Tamura et al. 1981; Roof et al. 2001) as before (Mostany et al. 2010), in order to compare both studies and also because the mechanism of neuronal injury (ischemia from arterial occlusion) is the same as the most common stroke pattern in humans (Lloyd-Jones et al. 2009). We focused our studies on the primary somatosensory cortex (S1) because it is commonly affected by stroke in humans, and because many studies addressing functional and structural plasticity in mice, including those investigating experience-dependent spine plasticity with in vivo two-photon microscopy, studied S1 (Holtmaat and Svoboda 2009).

Cranial windows for imaging spines in vivo were deliberately implanted in the contralesional hemisphere (Fig. 1*A*), so we could image neurons in homotopic areas of cortex corresponding to those that were destroyed by the infarct. MCAO produced moderate size infarcts (Fig. 1*B*), which spared the HP representation but included the lateral barrel field, rostral vibrissae, lower lip, and the forelimb portions of S1, as well as a small part of the rostrolateral primary motor cortex (Mostany et al. 2010). We selected the thy1 GFP-M line of transgenic mice because they express GFP sparsely in L5 pyramidal neurons, which makes it easier to image unobscured dendrites (Fig. 1*D*,*E*).

In humans, the majority of clinical improvement occurs in the first 3 months after stroke (Skilbeck et al. 1983). In rodents, the recovery is even faster, particularly when rehabilitative strategies are initiated within 2 weeks after stroke (Biernaskie et al. 2004). We have previously shown that mice subjected to distal MCAO exhibit signs of functional impairment, as manifested by reduced use of the contralateral forelimb in the cylinder test at +1 and +5 days after stroke, but significant functional recovery was observed in affected mice by +21 days post-stroke (Mostany et al. 2010). Thus, if the contralateral cortex plays a significant role in post-stroke recovery, it must do so within a few weeks after the initial insult. For this reason, we focused our imaging experiments on the first month after stroke, and mice were imaged every 4 days for ~40 days, including 3 baseline imaging sessions before the MCAO (Fig. 1*F*).

High-resolution two-photon microscopy allowed us to follow individual dendritic segments longitudinally before and after MCAO. We could not detect differences in spine density at any point after MCAO compared with the basal conditions (0.36 ± 0.09 spines/μm before vs. 0.34 ± 0.08 spines/μm after stroke; one-way ANOVA with repeated measures $P = 0.125$; Fig. 2*B*; 13 dendritic segments from 9 different L5 neurons in 4 mice). Structural rewiring may involve changes in spine dynamics without a change in spine density. For example, experience-dependent plasticity is associated with changes in spine turnover, even though spine density is unaffected (Holtmaat et al. 2006; Hofer et al. 2009). Therefore, we quantified the fraction of spines gained and lost between imaging sessions, as well as the density of transient spines (those appearing in only one imaging session), but found no differences in any of these parameters after stroke (one-way ANOVA with repeated measures $P = 0.192$, $P = 0.46$, $P = 0.277$, respectively; Fig. 2*C*–*E*). Next, we measured the probability that new spines would be stabilized because this parameter has been found to increase after whisker deprivation (Wilbrecht et al. 2010), which would suggest that new spines are permanently altering circuits after stroke. However, the spine stabilization probability (# new spines that persist for 3–5 imaging time points/# total new spines) was not significantly different in stroke versus control animals at any point after stroke (on average 0.36 ± 0.26 in stroke animals and 0.38 ± 0.34 in control animals; +4 to +20 days after MCAO; two-way ANOVA with repeated measures $P > 0.197$; Fig. 2*F*; control data come from 31 dendritic segments from 14 different L5 neurons in 8 control mice). Finally, we found that the survival function of spines did not change abruptly after stroke (Fig. 2*G*) and was similar to that of normal adult wild-type mice imaged in vivo (Holtmaat et al. 2006, 2009; Mostany et al. 2010; Wilbrecht et al. 2010). Also, there was no significant difference in the survival fraction of spines between the baseline period and the first 8 days after stroke (74.7 ± 9.9% for 8 days baseline vs. 83.3 ± 13.6% after 8 days post-stroke; $P = 0.101$; Fig. 2*G*, inset). Thus, L5 neurons in the contralateral cortex neither add nor retain spines after stroke to compensate for the massive loss of synapses in the lesioned hemisphere.

We also wondered whether, even in the absence of synaptic plasticity at the level of spines, stroke might have triggered large-scale remodeling of dendrites in the contralateral cortex to allow for new connections to be made. Previous Golgi studies have shown that after cortical lesions dendritic complexity of L5 pyramidal neurons increases in the spared

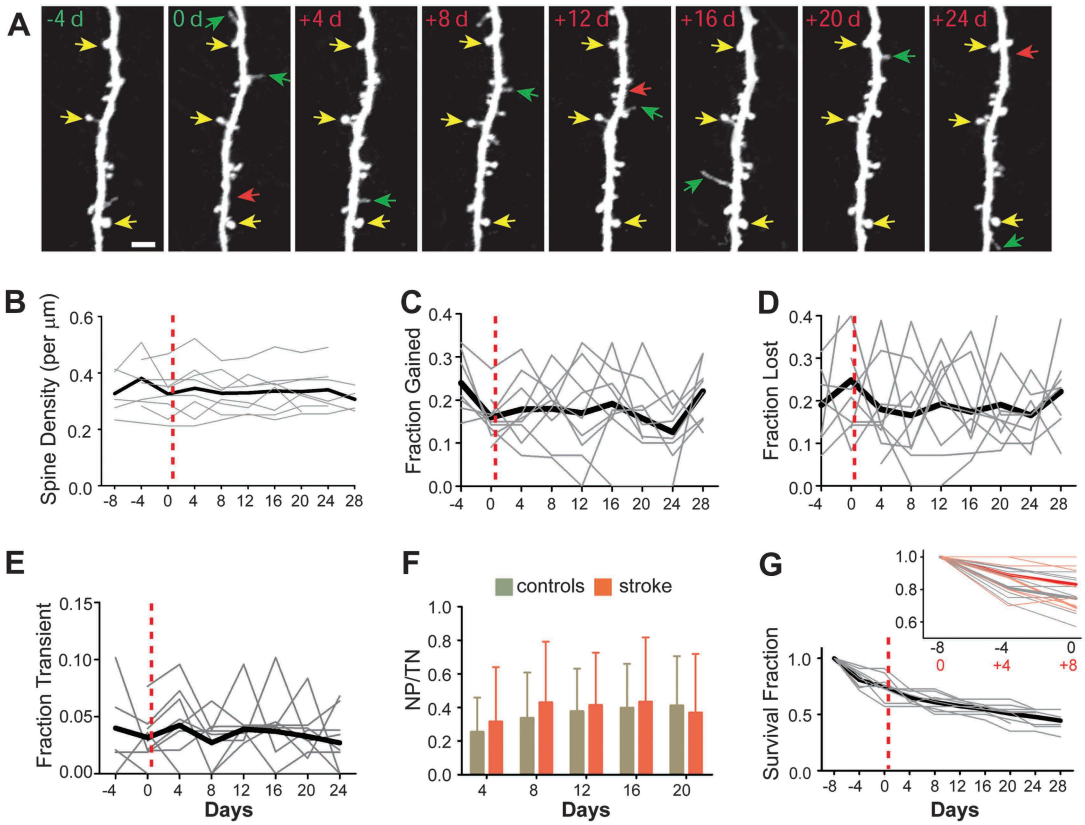

Figure 2. Chronic imaging of dendritic spines in contralateral cortex before and after MCAO shows no evidence of structural plasticity. (*A*) High-resolution two-photon images acquired in vivo of a typical apical dendritic segment from an L5 pyramidal neuron in the contralateral cortex before and after MCAO. All are maximum intensity projections (4–12 slices, 1.5 µm apart). A few examples of always present spines (yellow arrows), gained spines (green arrowheads), and lost spines (open red arrowheads) are shown. The day of imaging is shown in the upper left-hand corner (scale bar = 4 µm). (*B*) Normalized spine density over time for 9 L5 pyramidal neurons from 4 mice. Gray lines represent individual cells, and the thick black line is the average in panels (*B–E,G*). The vertical dashed line in panels (*B–E,G*) indicates the time of the MCAO. No significant change in spine density was found (one-way ANOVA with repeated measures $P = 0.125$). (*C* and *D*) Fraction of spines gained (*C*) and lost (*D*) over the total number of spines, as a function of time before and after MCAO. No statistical significance was found for either parameter before versus after MCAO (one-way ANOVA with repeated measures $P = 0.192$ and $P = 0.46$, respectively). (*E*) Fraction of transient spines (i.e., new spines that appeared on only one imaging time point and then disappeared; one-way ANOVA with repeated measures, $P = 0.28$). (*F*) Probability of new spine stabilization (a.k.a., spine stabilization ratio). The stabilization ratio was calculated as the number of new persistent spines (spines surviving 3 or more time points) divided by the total number of spines. No significant difference was found between the stabilization ratio of stroke group and a control group ($P = 0.197$). (*G*) Survival fraction of dendritic spines over time. The inset compares the survival fraction over the baseline time period (gray) and over the first 8 days after stroke (red). No significant change in survival fraction was found ($P = 0.101$).

hemisphere (Jones and Schallert 1992), particularly after rehabilitation (Jones and Schallert 1994; Biernaskie et al. 2004). However, others did not find any large-scale dendritic growth after cortical lesions (Forgie et al. 1996; Prusky and Whishaw 1996). The idea that pyramidal dendrites grow after brain injury is not supported by more recent in vivo imaging studies. For example, dendritic arbors of L5 pyramidal neurons appear to be stable in adult mice under normal conditions (Trachtenberg et al. 2002; Lee et al. 2006), suggesting that dendrites may not have the ability to grow at all in mature animals. In agreement with this notion, our previous longitudinal in vivo imaging study showed that dendrites of L5 pyramidal neurons in peri-infarct cortex did not grow or add new branches after MCAO stroke (Mostany and Portera-Cailliau 2011). We measured the changes in length of 11 dendritic tips from 7 neurons of 4 mice (average tip segment length was 24 µm) after stroke and found no evidence for dendrite remodeling, as the tip length did not change significantly before or after stroke (on average −1.2 ± 1.5 µm after stroke vs. −0.4 ± 0.8 µm at baseline, one-way ANOVA with repeated measures, $P = 0.159$; Fig. 3).

No Functional Remapping in Contralateral Cortex of Adult Mice

It is possible that the contralateral cortex might exhibit functional remapping in the absence of structural rewiring at the level of pyramidal dendrites. Thus, we next chose to explore a functional readout of cortical plasticity and investigate the potential remapping of sensory-evoked cortical activity to the contralateral hemisphere after stroke. In addition, we wanted to test the biphasic theory of remapping, which suggests that remapping first involves the spared hemisphere (in the first few days after stroke) until the peri-infarct cortex can be recruited later after the initial ischemic insult subsides (Marshall et al. 2000; Dijkhuizen et al. 2001, 2003). That pioneering work in humans and rats using functional magnetic resonance imaging (fMRI) suffers from limited temporal and spatial resolution. In most cases, these were not longitudinal studies, and subjects after stroke recovery were compared with normal controls. Therefore, we used longitudinal IOS imaging to record the cortical regions that respond to sensory stimulation of the contralateral and ipsilateral (affected) FP before and after stroke.

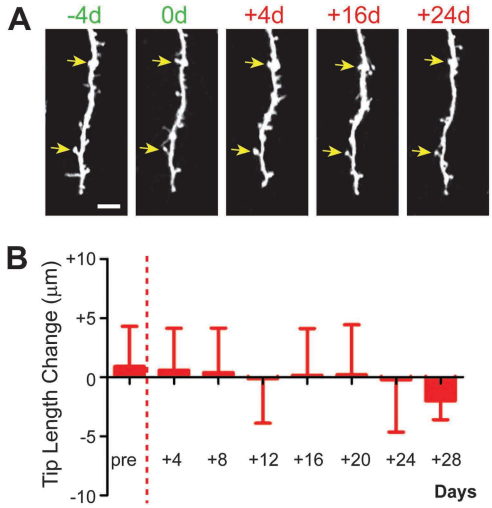

Figure 3. Absence of large-scale plasticity in contralateral cortex after MCAO. (*A*) Representative two-photon images of the same tip of an apical dendrite from a L5 pyramidal cell in the contralateral cortex before and after the stroke (best projections of image stacks consisting of 5–10 slices, 1.5 µm apart). (*B*) Changes in dendritic tip length over time. Length was measured from fiducial points that could be identified at every time point before and after MCAO (stable spines; yellow arrows). No significant growth or retraction of tips was seen after the stroke (one-way ANOVA with repeated measures, $P = 0.159$).

Due to variations in the intracerebral arterial anatomy from mouse to mouse, the exact infarct size and location after MCAO is somewhat variable, and this could confound the results of IOS mapping. For these reasons, we also used the Rose Bengal photothrombotic (RBPT) stroke model, so we could specifically produce an infarct of consistent size that was targeted to the FP region and then image the exact homotopic cortical area in the contralateral spared hemisphere. The main criticism of the RBPT model has been that both veins and arteries are occluded, and there is virtually no reperfusion from collaterals. This was not a problem for our experiments because we investigated the mechanisms of plasticity in the homotopic cortex, the drive for which is presumably triggered by ischemic cortical injury in the opposite hemisphere, regardless of mechanism. A halogen lamp coupled to a fiber-optic guide probe was used to focus white light on a 2.75 mm diameter area over S1FL (Fig. 4*A*) to create a focal infarct spanning all layers of the neocortex but sparing subcortical regions (Fig. 4*B*).

After the last imaging session, all mice were perfusion-fixed with 4% paraformaldehyde, and brains were stained with cresyl violet to confirm the location and size of the infarct. An advantage of investigating functional remapping with 2 different stroke models was that we could test the theory that small strokes trigger remapping in peri-infarct cortex, whereas large strokes are more likely to recruit the contralateral hemisphere (Abo et al. 2001; Calautti et al. 2001; Biernaskie et al. 2004; Cramer and Crafton 2006). However, although the volume of RBPT infarcts was smaller than that of MCAO infarcts (2.7 ± 1.6 mm^3 for RBPT vs. 4.8 ± 1.4 mm^3 for MCAO; Fig. 4*C*), they were directly targeted to the FP representation.

Mice were imaged at a baseline before stroke and then again at +1, +3, +5, +7, +14, and +21 days after stroke. For every imaging session, we acquired IOS signals during stimulation of each FP individually. There was no difference in IOS map size or signal intensity change between MCAO and RBPT stroke models (two-way ANOVA with repeated measures; $P = 0.091$ and $P = 0.354$, respectively; $n = 4$ each; not shown), so both sets of data were pooled for analysis. Stimulation of the FP contralateral to the imaging window reproducibly evoked a detectable IOS signal in the expected location in S1FL (Diamond et al. 1999; Grove and Fukuchi-Shimogori 2003; Winship and Murphy 2008), and this map did not change in location after MCAO or RBPT stroke (Fig. 4*D*,*E*, images on the left). As expected, in the baseline imaging session, we could not detect an IOS map by stimulating the affected FP ipsilateral to the imaging window (Fig. 4*D*, images on the right). Even after stroke, however, IOS imaging did not reveal an activity map after stimulation of the ipsilateral (affected) FP in the spared cortex (Fig. 4*E*, images on the right).

Quantitative analysis revealed that the area of IOS maps elicited by contralateral stimulation was significantly different from that elicited by ispilateral stimulation at every time point before and after stroke (intercept test, $P < 0.01$; Fig. 4*F*, $n = 8$ mice). Thus, although contralateral FP stimulation consistently evoked activity maps of 0.5–2 mm^2 in the spared S1FL (on average 1.06 mm^2), the map area after ipsilateral stimulation was not significantly different from zero at any time point (intercept test, $P > 0.05$). In addition, although there was a trend toward a larger IOS map following contralateral stimulation at +5 days after stroke compared with baseline, the difference was not statistically significant. Thus, although some mice in our study showed what look like disinhibition of FP-evoked responses in the contralesional hemisphere after stroke (Fig. 4*F*), as recently described using voltage sensitive dye (VSD) imaging (Mohajerani et al. 2011), using IOS imaging, we could not detect this phenomenon across all animals in our study.

We also quantified the % signal intensity change over background before and after stroke in IOS maps elicited by contralateral and ipsilateral FP stimulation (Fig. 4*G*). To avoid any bias in selecting IOS maps, we calculated a signal-over-background ratio by dividing the average pixel intensity of the IOS images in the presumed region of the FP map (based on the contralateral stimulation map; see Materials and Methods) by the average pixel intensity of an ROI of equal size located outside of the FP map (see Materials and Methods). The % signal change for the FP map evoked by contralateral stimulation varied slightly between sessions from 2% to 17% (due to inherent variability in chronic IOS measurements) and was significantly higher than the % signal change for the FP map after ipsilateral stimulation (intercept test, $P < 0.01$; Fig. 4*G*). The signal change after ipsilateral stimulation was always less than 1% and did not change significantly after stroke ($P > 0.05$). We conclude that sensory stimulation of ipsilateral FP does not elicit an evoked response in S1FL that can be detected with IOS imaging up to 3 weeks after stroke.

It is possible that the sensitivity of IOS imaging through the skull was not sufficient to detect very small or weak signals from ipsilateral FP stimulation in the contralateral hemisphere. As a control, we used IOS to record the whisker representations. At baseline, we were able to detect IOS signals resulting from contralateral stimulation of just a single whisker. Stimulation of the D2 whisker resulted in maps in the contralateral hemisphere with an average area of 0.23 mm^2 (not shown; $n = 4$ mice). This represents ~22% of the size of the average map that results from contralateral FP stimulation. Thus, we were able to detect rather small maps with our IOS technique. In a different group of mice, we also investigated

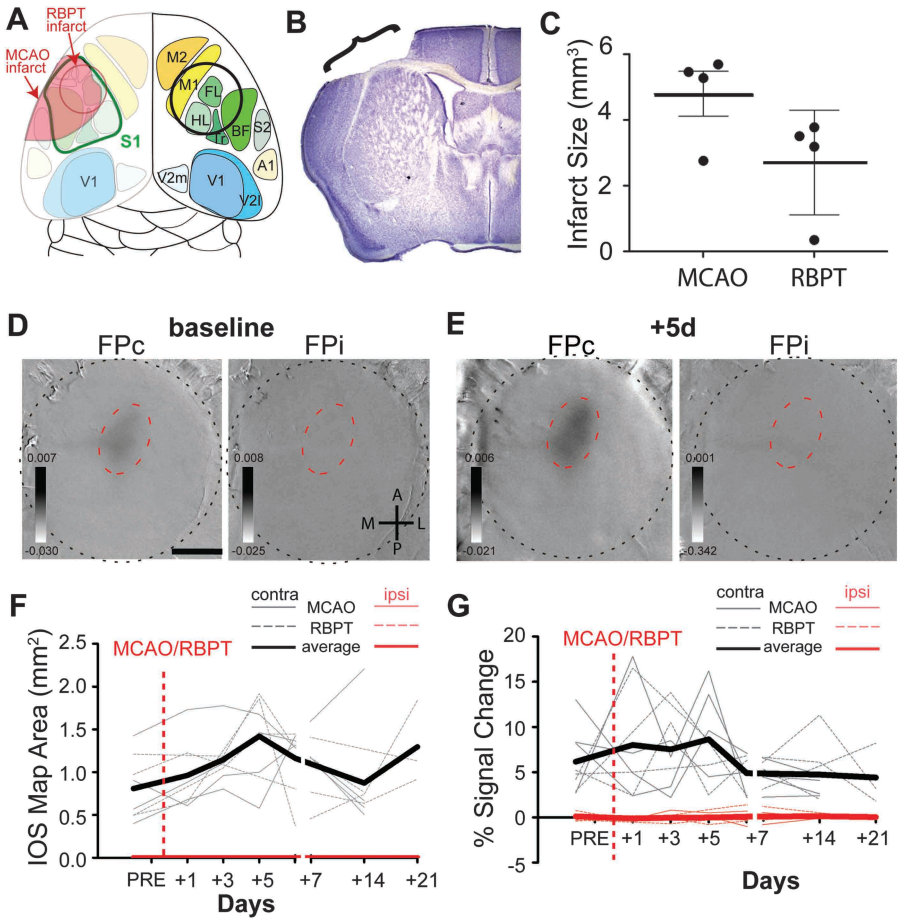

Figure 4. IOS experiments in adult mice show no evidence of functional remapping in the contralateral cortex after MCAO or RBPT stroke. (*A*) Location of the cranial window in relationship to functional brain regions (adapted from Diamond et al. 1999; Grove and Fukuchi-Shimogori 2003; Van der Gucht et al. 2007). Green shading is for primary somatosensory cortex (BF: barrel field; FL: forelimb; HL: hindlimb; LL: lower lip; No: nostril; Rv: rostral vibrissae; Tr: trunk; and UL: upper lip), blue shading is for visual cortex, and red shading for motor cortex. (*B*) Mid coronal section (at the level of Bregma) stained with cresyl violet from an adult mouse in this study, showing the location and size of a representative infarct induced by focal RBPT. (*C*) Volume of infarcts for animals used for IOS experiments. (*D*) Baseline IOS images after stimulation of the contralateral (FPc, left) and ipsilateral (FPi, right) in a representative mouse. A: anterior; P: posterior; L: lateral; and M: medial. The dashed black circle outlines the window area and the dashed red oval outlines the actual FPc map area in S1FL. Insets in each image show raw change in reflectance after FP stimulation. No map was detected during stimulation of the FPi. Scale bar (1 mm) is the same for panel *F*. (*E*) IOS images for the same animal 5 days after stroke corresponding to stimulation of the FPc (left) and FPi (right). (*F*) IOS map size (area in mm^2) corresponding to a 62.5% threshold of the maps resulting from stimulation of the FPc (solid gray line is after MCAO and dashed gray line is after RBPT) and FPi (red) over time before and after stroke. For analysis, data for MCAO and RBPT infarcts were pooled together, and the average is shown in black. Ipsilateral stimulation resulted in a map area that was not significantly different from zero, but the difference between ipsilateral and contralateral stimulation was significant at all time points before and after stroke (intercept test $P > 0.05$ and $P < 0.01$, respectively). (*G*) Percent change in signal intensity for IOS maps corresponding to stimulation of the FPi (pink lines; average shown in red) and FPc (gray lines; average shown in black) over time before and after stroke. The magnitude of the IOS signal was quantified by taking the ratio of the average pixel value within the expected FPc map area (dashed red oval in *E* and *F*) divided by the average pixel value of an equal sized area just outside the FPc map area. This provided a measure of the strength of the IOS signal against the background level of noise. There was no significant IOS signal after FPi stimulation (intercept test $P > 0.05$).

whether we could detect remapping in peri-infarct cortex with IOS imaging through the skull. We found that the WS map disappeared acutely after stroke but then reappeared by +13 days in a new location (not shown). The medial–caudal displacement of the WS map after stroke was significantly greater than the average movement of the map with repeated measurements during the baseline period before the stroke (1.01 ± 0.34 mm after stroke vs. 0.15 ± 0.08 mm at baseline; $P < 0.01$; $n = 2$ mice). The remapped representation was of equivalent signal intensity to the original map in barrel cortex.

Lack of Functional Remapping in Contralateral Cortex of Juvenile Mice

Children recover from brain lesions, including stroke, more fully than adults (deVeber et al. 2000; Ganesan et al. 2000; Kim et al. 2009). Therefore, we hypothesized that young mice might exhibit cortical remapping after MCAO stroke in the contralateral hemisphere. To test this, we implanted cranial windows in juvenile mice and induced infarcts at postnatal day (P) 19–P24 and then carried out IOS imaging before and at +1, +3, +7, and +14 days after an MCAO stroke. In juvenile mice, the unilateral distal MCAO also produced infarcts that included the FP representation in S1FL, but their size was more variable than in adult mice (not shown). The first baseline IOS imaging session was usually done 1–2 days after implanting the cranial window, and this was followed 2–3 days later by MCAO surgery. In Juvenile mice, distinct maps could also be evoked by stimulation of the contralateral FP before and after stroke (Fig. 5*B*,*D*), and the size of thresholded maps was similar to that of maps in adults (on average 0.98 ± 0.31 mm^2 in juvenile vs. 1.13

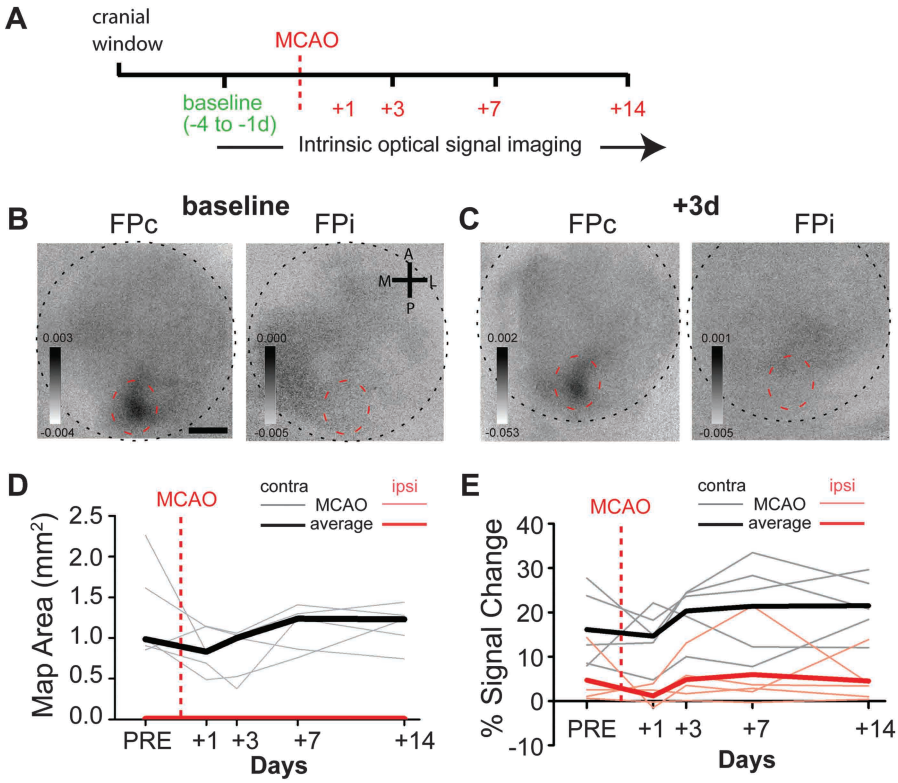

Figure 5. IOS experiments in juvenile mice show no evidence of functional remapping in the contralateral cortex after MCAO stroke. (*A*) Timeline of IOS imaging experiments in juvenile mice with respect to the time of stroke (dashed red line). Baseline images were taken at P18, and the infarct was induced at P19–P21. (*B*) Baseline IOS images after stimulation of the contralateral (FPc, left) and ipsilateral (FPi, right) in a representative mouse. A: anterior; P: posterior; L: lateral; and M: medial. The dashed black circle outlines the window area and the dashed red oval outlines the actual FPc map area in S1FL. Insets in each image show raw change in reflectance after FP stimulation no map was detected during stimulation of the FPi. Scale bar (1 mm) is the same for panel *C*. (*C*) IOS images for the same animal 3 days after stroke corresponding to stimulation of the FPc (left) and FPi (right). (*D*) IOS map size (area in mm^2) corresponding to a 62.5% threshold of the maps resulting from stimulation of the FPc (gray) and FPi (red) over time before and after MCAO stroke. The bold black/red lines are the average of 5 mice. Note that the FPi map size was never significantly different from zero after ipsilateral stimulation (intercept test $P > 0.05$). (*E*) Percent change in signal intensity for IOS maps corresponding to stimulation of the FPi (pink lines; average in red) and FPc (gray lines; average in black) over time before and after MCAO. The difference in signal change was always significant between ipsilateral and contralateral stimulation (intercept test $P < 0.01$).

± 0.47 mm^2 in adults; Figs 4*F* and 5*D*). Just as with adult animals, using IOS imaging, we could not detect activity maps that were significantly different from zero after ipsilateral FP stimulation at any point before or after stroke in juvenile mice (intercept test, $P > 0.05$; Fig. 5*C,D*). In juvenile mice, we again found that the magnitude of IOS signal change in the spared hemisphere was significantly greater after contralateral stimulation than after ipsilateral stimulation in juvenile animals (on average 16 ± 9% change for contralateral vs. 5 ± 6% change for ipsilateral; intercept test $P > 0.05$; Fig. 5*E*). Furthermore, the signal change after ipsilateral stimulation did not change significantly after stroke (4.7 ± 5.6% for the –1 day baseline vs. 4.1 ± 4.7% for the +1 to +14 days post-stroke average; $P > 0.05$).

Discussion

Lack of Dendritic Plasticity after Stroke: A Controversy Resolved?

One of the goals of the structural imaging portion of our study was to resolve the long-standing and contentious debate regarding the role of dendritic plasticity after unilateral cortical injury in the contralateral cortex. Previously, some Golgi studies found evidence for major remodeling of dendrites of pyramidal neurons after focal cortical lesions (Jones and Schallert 1992, 1994), while others found no change in dendritic structure (Forgie et al. 1996; Prusky and Whishaw 1996). But those studies suffered from potential selection bias because different neurons from different animals were pooled for each experimental time point before and after stroke. Indeed, since the Golgi method can be somewhat capricious in its staining, it is possible that slightly different neuronal subtypes were labeled and analyzed in different groups. In addition, the static snapshots of Golgi-stained neurons in fixed tissue could not provide information regarding dynamic changes in dendritic arbors and spines, which could be critical elements of neural repair after stroke. To overcome those limitations, we used high resolution in vivo chronic two-photon microscopy to image the same dendrites before and after stroke in a homogeneous population of GFP-expressing L5 pyramidal neurons. Thus, major strengths of our approach were the fact that each neuron served as its own control and also that we could record dynamic rearrangements of dendritic structure.

We found no evidence of de novo growth or branching of dendrites in the spared cortex after stroke, which is in agreement with some of the more recent studies in fixed tissue (Biernaskie et al. 2004; Gibb et al. 2010). In a previous study, we had similarly found no evidence of large-scale dendritic plasticity

in peri-infarct cortex after stroke (Mostany and Portera-Cailliau 2011). Considering the natural tendency of pyramidal neuron dendrites in adult mice to remain stable over periods of months (Trachtenberg et al. 2002; Lee et al. 2006; Mostany and Portera-Cailliau 2011), we conclude that pyramidal neurons are not capable of elongating their dendrites or growing new dendritic branches to compensate for ischemic brain damage in mature animals.

In addition, we did not find any plasticity at the level of dendritic spines, in contrast to what has previously been reported in peri-infarct cortex (Brown et al. 2007, 2009; Mostany et al. 2010). Our spine data differ from that in a recent in vivo two-photon imaging study of dendritic spine dynamics of L5 pyramidal neurons in the contralateral cortex after stroke (Takatsuru et al. 2009). In that paper, the authors reported an increase in the turnover rate of mushroom spines over 6 h at 1 week after stroke. We used 4 days intervals for imaging spines because several studies have shown that this corresponds to the average half-life of the most dynamic spines in the adult mouse S1 cortex and also because the least stable thin spines and filopodia, which represent a small fraction of all spines, only rarely transform into persistent mushroom spines (Holtmaat et al. 2005; Zuo et al. 2005). Thus, although it is possible that over very short intervals (6 h instead of 4 days) dendritic spines of neurons in the contralateral cortex may be plastic after stroke, the impact of this plasticity in rewiring circuits seems negligible. Another difference was that in their cross-sectional study, Takatsuru et al. (2009) examined different animals at different time points after stroke, unlike our longitudinal survey that followed the same neurons before and after stroke. They also used a different mouse line (YFP-H) and the RBPT stroke model, so differences in the experimental approach could also explain the different results.

Overall, we conclude that, in contrast with the dramatic changes in spine density and turnover in peri-infarct cortex (Mostany et al. 2010), L5 pyramidal neurons in the spared hemisphere do not participate significantly in compensatory plasticity after stroke. The lack of spine plasticity also implies that axons that are presynaptic to those spines are unlikely to exhibit significant rewiring after stroke. Nonetheless, the fact that we did not observe any large-scale or spine remodeling in apical dendrites of L5 pyramidal neurons does not necessarily mean that the homotopic contralateral cortex does not rewire after stroke. Additional studies will be necessary to investigate whether apical or basal dendrites (or axons) of neurons in other cortical layers in the spared hemisphere, including cortical interneurons (which are inherently more plastic than those of pyramidal neurons in adult mice; Lee et al. 2006), exhibit structural plasticity.

No Functional Remapping to the Contralateral Homotopic Cortex after Stroke in Adult or Juvenile Mice

Over the last 3 decades, many functional brain imaging studies in rats and humans have investigated the remapping of lost functionalities to related brain areas in both hemispheres. Most studies found extensive activation of regions in the ipsilesional hemisphere, but a few also provided evidence of contralateral remapping after stroke (Chollet et al. 1991; Weiller et al. 1992; Seitz et al. 1998; Marshall et al. 2000; Abo et al. 2001; Calautti et al. 2001; Dijkhuizen et al. 2001; Rossini et al. 2003; Ward 2004; Schaechter and Perdue 2008). However, there are also published reports finding no remapping in the spared hemisphere (Tuor et al. 2007; Weber et al. 2008), so the extent to which the contralateral plasticity contributes to functional recovery after stroke has not yet been fully established. Naturally, the majority of the past studies in humans were cross-sectional, meaning that only fully recovered stroke patients were imaged, and results were compared with normal adults rather than to a pre-stroke baseline (Calautti and Baron 2003). Our in vivo chronic IOS imaging approach aimed to overcome this limitation because it allowed us to follow the same mice before and after stroke, so we could investigate the time course of ipsi- and contralateral remapping. Furthermore, because IOS imaging has better spatial resolution than fMRI or positron emission tomography, we could reliably identify response maps as small as 0.23 mm^2 in size, and we were positioned to detect even the slightest signs of contralesional activation.

Surprisingly, we could not find any evidence of functional remapping to the spared hemisphere after stroke in adult mice over a period of 3 weeks after stroke. Whether some remapping occurs, there at later time points remains to be seen, but if that were the case, such delayed contralateral plasticity could not easily explain the behavioral recovery. Indeed, even though the majority of recovery in human stroke victims occurs within the first 3 months (Skilbeck et al. 1983), recovery in rodents is much quicker (Biernaskie et al. 2004; Brown et al. 2007; Mostany et al. 2010). It has been proposed that the contralateral cortex may only participate in reparative plasticity after very large strokes (Murphy and Corbett 2009), and although our models produce moderate size infarcts, perhaps recruitment of the spared hemisphere requires more overwhelming brain insults.

In addition, because children can recover more quickly and to a greater extent after cortical injury (Johnston 2009; Kim et al. 2009), we also examined whether juvenile mice might be better equipped than adults to manifest functional remapping in the contralateral cortex. However, stimulation of the affected FP did not elicit any detectable IOS map in the spared hemisphere even in 3-week-old mice. In summary, we conclude that, at least in mice, the spared cortex does not play a significant role in functional remapping in the first month after stroke.

Taking into account that IOS imaging is not as sensitive as electrophysiological or calcium imaging approaches for detecting sensory-evoked responses, it is conceivable that this limitation could explain why we did not detect ipsilateral responses even during the baseline period before stroke. For example, an in vivo calcium imaging study of layer 2/3 neurons in adult mice found rare cells that responded to ipsilateral FP stimulation (Winship and Murphy 2008). Another study that used spectral imaging reported small decreases in oxygenation after ipsilateral stimulation of the FP in rats compared with large increases in oxygenation/flow after contralateral stimulation (Devor et al. 2008). In contrast, using a similar IOS approach to ours through a glass-covered cranial window in mice, the Murphy lab did not detect an ipsilateral response with FP stimulation (Winship and Murphy 2008). Interestingly, using VSD imaging, the same lab found that FP stimulation produced responses that spread from the contralateral cortex to the mirror area in the ipsilateral hemisphere (Mohajerani et al. 2011). The ipsilateral VSD signals were weaker and likely represented subthreshold neuronal activity. Our control IOS experiments show that we can detect maps elicited by contralateral stimulation of a single whisker,

which are ~20% as large as the FP maps. Still, it is possible that if contralateral remapping after stroke led to a much more subtle ipsilateral response to FP stimulation, this could result in changes in laterality that favor ipsilateral responses in the spared hemisphere since the contralateral responses are virtually absent in peri-infarct cortex (Dijkhuizen et al. 2001).

Is Contralateral Plasticity Maladaptive?

Whether the contralateral cortex contributes to functional recovery after stroke is an important question because stroke remains the leading cause of adult disability in North America and a better understanding of the mechanisms of neuronal plasticity after brain injury should result in improved rehabilitative interventions, not only just for motor deficits but also for other debilitating symptoms, such as aphasia or cognitive impairment. Intuitively, the homotopic cortex in the spared hemisphere presents itself as an ideal place for adaptive plasticity because it is not affected by ischemia or inflammation after stroke and because it is already wired to perform identical functions as the infarcted tissue, but for the opposite side of the body. The evidence from previous functional imaging studies demonstrating remapping of lost functionalities to the contralateral cortex had made this argument even more compelling. In addition, some studies using transcranial magnetic stimulation to disrupt activity within the contralesional dorsal premotor cortex (an area of presumed remapping) demonstrated worse performance during a recovered hand movement (Lotze et al. 2006).

Our data, however, argue against a role of the contralateral cortex in functional recovery after stroke. Other studies suggest that remapping to the unaffected hemisphere may only happen in stroke patients with slow and/or poor recovery (Carey et al. 2002; Fujii and Nakada 2003; Murphy and Corbett 2009). Together, these findings raise the possibility that contralateral recruitment after stroke may be a last ditch effort, or worse yet, a maladaptive form of plasticity. The theme that emerges is that the greater involvement of the ipsilesional cortex in plasticity, the better the recovery (Calautti and Baron 2003).

In the context of functional recovery after stroke, the main goal is to restore lost functions. In most cases, this involves retraining new brain regions to overcome sensorimotor deficits. As patients recover, they are generally not performing the lost capability (e.g., language, motor function) in the same fashion as before the stroke. Even for rodents performing a skilled reaching task, there is evidence that the manner in which the animal performs the task is significantly different after stroke (Tennant and Jones 2009). The animal appears to adapt by using other parts of its body such as the unaffected paw and postural muscles to compensate, which implies plasticity in nearby regions within the peri-infarct cortex. This argues strongly against a model where lost functionalities are simply transferred to the contralateral homotopic region. Instead, it suggests that functional recovery is due to recruitment of other sensorimotor areas in the affected hemisphere. This explanation seems all the more reasonable in the absence of an obvious mechanism for how the rewiring of a sensory pathway to a new hemisphere might occur over such a rapid timeframe. Future studies will need to address this further, perhaps by correlating functional remapping to different brain regions with behavioral recovery.

Funding

National Institute for Childhood and Developmental Disorders (grant 5R01HD054453 to C.P.C.); Larry L Hillblom Foundation (to C.P.C.); March of Dimes Foundation (grant 1-FY06-357 to C.P.C.).

Notes

We thank Drs Adrian Cheng and J. Tiago Gonçalves for help with analysis of IOS signals in MATLAB, Dr Alan Garfinkel for help with statisitcs, members of the lab for helpful comments on the manuscript, and Dr S. Thomas Carmichael, Dean Buonomano, and Felix Schweizer for guidance at various stages of this project. *Conflict of Interest*: None declared.

References

Abo M, Chen Z, Lai LJ, Reese T, Bjelke B. 2001. Functional recovery after brain lesion—contralateral neuromodulation: an fMRI study. Neuroreport. 12:1543–1547.

Biernaskie J, Chernenko G, Corbett D. 2004. Efficacy of rehabilitative experience declines with time after focal ischemic brain injury. J Neurosci. 24:1245–1254.

Brown CE, Aminoltejari K, Erb H, Winship IR, Murphy TH. 2009. In vivo voltage-sensitive dye imaging in adult mice reveals that somatosensory maps lost to stroke are replaced over weeks by new structural and functional circuits with prolonged modes of activation within both the peri-infarct zone and distant sites. J Neurosci. 29:1719–1734.

Brown CE, Li P, Boyd JD, Delaney KR, Murphy TH. 2007. Extensive turnover of dendritic spines and vascular remodeling in cortical tissues recovering from stroke. J Neurosci. 27:4101–4109.

Calautti C, Baron JC. 2003. Functional neuroimaging studies of motor recovery after stroke in adults: a review. Stroke. 34:1553–1566.

Calautti C, Leroy F, Guincestre JY, Marie RM, Baron JC. 2001. Sequential activation brain mapping after subcortical stroke: changes in hemispheric balance and recovery. Neuroreport. 12:3883–3886.

Cao Y, George KP, Ewing JR, Vikingstad EM, Johnson AF. 1998. Neuroimaging of language and aphasia after stroke. J Stroke Cerebrovasc Dis. 7:230–233.

Carey JR, Kimberley TJ, Lewis SM, Auerbach EJ, Dorsey L, Rundquist P, Ugurbil K. 2002. Analysis of fMRI and finger tracking training in subjects with chronic stroke. Brain. 125:773–788.

Chollet F, DiPiero V, Wise RJ, Brooks DJ, Dolan RJ, Frackowiak RS. 1991. The functional anatomy of motor recovery after stroke in humans: a study with positron emission tomography. Ann Neurol. 29:63–71.

Cramer SC, Crafton KR. 2006. Somatotopy and movement representation sites following cortical stroke. Exp Brain Res. 168:25–32.

deVeber GA, MacGregor D, Curtis R, Mayank S. 2000. Neurologic outcome in survivors of childhood arterial ischemic stroke and sinovenous thrombosis. J Child Neurol. 15:316–324.

Devor A, Hillman EM, Tian P, Waeber C, Teng IC, Ruvinskaya L, Shalinsky MH, Zhu H, Haslinger RH, Narayanan SN, et al. 2008. Stimulus-induced changes in blood flow and 2-deoxyglucose uptake dissociate in ipsilateral somatosensory cortex. J Neurosci. 28:14347–14357.

Diamond ME, Petersen RS, Harris JA. 1999. Learning through maps: functional significance of topographic organization in primary sensory cortex. J Neurobiol. 41:64–68.

Dijkhuizen RM, Ren J, Mandeville JB, Wu O, Ozdag FM, Moskowitz MA, Rosen BR, Finklestein SP. 2001. Functional magnetic resonance imaging of reorganization in rat brain after stroke. Proc Natl Acad Sci U S A. 98:12766–12771.

Dijkhuizen RM, Singhal AB, Mandeville JB, Wu O, Halpern EF, Finklestein SP, Rosen BR, Lo EH. 2003. Correlation between brain reorganization, ischemic damage, and neurologic status after transient focal cerebral ischemia in rats: a functional magnetic resonance imaging study. J Neurosci. 23:510–517.

Feng G, Mellor RH, Bernstein M, Keller-Peck C, Nguyen QT, Wallace M, Nerbonne JM, Lichtman JW, Sanes JR. 2000. Imaging neuronal subsets in transgenic mice expressing multiple spectral variants of GFP. Neuron. 28:41–51.

Forgie ML, Gibb R, Kolb B. 1996. Unilateral lesions of the forelimb area of rat motor cortex: lack of evidence for use-dependent neural growth in the undamaged hemisphere. Brain Res. 710: 249–259.

Fujii Y, Nakada T. 2003. Cortical reorganization in patients with subcortical hemiparesis: neural mechanisms of functional recovery and prognostic implication. J Neurosurg. 98:64–73.

Ganesan V, Hogan A, Shack N, Gordon A, Isaacs E, Kirkham FJ. 2000. Outcome after ischaemic stroke in childhood. Dev Med Child Neurol. 42:455–461.

Gibb RL, Gonzalez CL, Wegenast W, Kolb BE. 2010. Tactile stimulation promotes motor recovery following cortical injury in adult rats. Behav Brain Res. 214:102–107.

Glees P, Cole J. 1950. Recovery of skilled motor functions after small repeated lesions of motor cortex in macaque. J Neurophysiol. 13:137–148.

Grotta JC, Jacobs TP, Koroshetz WJ, Moskowitz MA. 2008. Stroke program review group: an interim report. Stroke. 39:1364–1370.

Grove EA, Fukuchi-Shimogori T. 2003. Generating the cerebral cortical area map. Annu Rev Neurosci. 26:355–380.

Hofer SB, Mrsic-Flogel TD, Bonhoeffer T, Hubener M. 2009. Experience leaves a lasting structural trace in cortical circuits. Nature. 457:313–317.

Holtmaat A, Bonhoeffer T, Chow DK, Chuckowree J, De Paola V, Hofer SB, Hubener M, Keck T, Knott G, Lee WC, et al. 2009. Long-term, high-resolution imaging in the mouse neocortex through a chronic cranial window. Nat Protoc. 4:1128–1144.

Holtmaat A, Svoboda K. 2009. Experience-dependent structural synaptic plasticity in the mammalian brain. Nat Rev Neurosci. 10:647–658.

Holtmaat A, Wilbrecht L, Knott GW, Welker E, Svoboda K. 2006. Experience-dependent and cell-type-specific spine growth in the neocortex. Nature. 441:979–983.

Holtmaat AJ, Trachtenberg JT, Wilbrecht L, Shepherd GM, Zhang X, Knott GW, Svoboda K. 2005. Transient and persistent dendritic spines in the neocortex in vivo. Neuron. 45:279–291.

Johnston MV. 2009. Plasticity in the developing brain: implications for rehabilitation. Dev Disabil Res Rev. 15:94–101.

Jones TA, Schallert T. 1992. Overgrowth and pruning of dendrites in adult rats recovering from neocortical damage. Brain Res. 581:156–160.

Jones TA, Schallert T. 1994. Use-dependent growth of pyramidal neurons after neocortical damage. J Neurosci. 14:2140–2152.

Kim CT, Han J, Kim H. 2009. Pediatric stroke recovery: a descriptive analysis. Arch Phys Med Rehabil. 90:657–662.

Lee WC, Huang H, Feng G, Sanes JR, Brown EN, So PT, Nedivi E. 2006. Dynamic remodeling of dendritic arbors in GABAergic interneurons of adult visual cortex. PLoS Biol. 4:e29.

Lim D, Mohajerani M, LeDue J, Boyd J, Chen S, Murphy T. 2012. In vivo large-scale cortical mapping using channelrhodopsin-2 stimulation in transgenic mice reveals asymmetric and reciprocal relationships between cortical areas. Front Neural Circuits. 6:11.

Lloyd-Jones D, Adams R, Carnethon M, De Simone G, Ferguson TB, Flegal K, Ford E, Furie K, Go A, Greenlund K, et al. 2009. Heart disease and stroke statistics—2009 update: a report from the American Heart Association statistics Committee and stroke statistics Subcommittee. Circulation. 119:480–486.

Lotze M, Markert J, Sauseng P, Hoppe J, Plewnia C, Gerloff C. 2006. The role of multiple contralesional motor areas for complex hand movements after internal capsular lesion. J Neurosci. 26:6096–6102.

Marshall RS, Perera GM, Lazar RM, Krakauer JW, Constantine RC, DeLaPaz RL. 2000. Evolution of cortical activation during recovery from corticospinal tract infarction. Stroke. 31:656–661.

Mohajerani MH, Aminoltejari K, Murphy TH. 2011. Targeted mini-strokes produce changes in interhemispheric sensory signal processing that are indicative of disinhibition within minutes. Proc Natl Acad Sci U S A. 108:E183–E191.

Mostany R, Chowdhury TG, Johnston DG, Portonovo SA, Carmichael ST, Portera-Cailliau C. 2010. Local hemodynamics dictate long-term dendritic plasticity in peri-infarct cortex. J Neurosci. 30:14116–14126.

Mostany R, Portera-Cailliau C. 2008. A craniotomy surgery procedure for chronic brain imaging. J Vis Exp. (12):pii: 680.

Mostany R, Portera-Cailliau C. 2011. Absence of large-scale dendritic plasticity of layer 5 pyramidal neurons in peri-infarct cortex. J Neurosci. 31:1734–1738.

Murphy TH, Corbett D. 2009. Plasticity during stroke recovery: from synapse to behaviour. Nat Rev Neurosci. 10:861–872.

Pologruto TA, Sabatini BL, Svoboda K. 2003. ScanImage: flexible software for operating laser scanning microscopes. Biomed Eng Online. 2:13.

Prusky G, Whishaw IQ. 1996. Morphology of identified corticospinal cells in the rat following motor cortex injury: absence of use-dependent change. Brain Res. 714:1–8.

Roof RL, Schielke GP, Ren X, Hall ED. 2001. A comparison of long-term functional outcome after 2 middle cerebral artery occlusion models in rats. Stroke. 32:2648–2657.

Rossini PM, Calautti C, Pauri F, Baron JC. 2003. Post-stroke plastic reorganisation in the adult brain. Lancet Neurol. 2:493–502.

Schaechter JD, Perdue KL. 2008. Enhanced cortical activation in the contralesional hemisphere of chronic stroke patients in response to motor skill challenge. Cereb Cortex. 18:638–647.

Seitz RJ, Hoflich P, Binkofski F, Tellmann L, Herzog H, Freund HJ. 1998. Role of the premotor cortex in recovery from middle cerebral artery infarction. Arch Neurol. 55:1081–1088.

Skilbeck CE, Wade DT, Hewer RL, Wood VA. 1983. Recovery after stroke. J Neurol Neurosurg Psychiatry. 46:5–8.

Takatsuru Y, Fukumoto D, Yoshitomo M, Nemoto T, Tsukada H, Nabekura J. 2009. Neuronal circuit remodeling in the contralateral cortical hemisphere during functional recovery from cerebral infarction. J Neurosci. 29:10081–10086.

Tamura A, Graham DI, McCulloch J, Teasdale GM. 1981. Focal cerebral ischaemia in the rat: 1. Description of technique and early neuropathological consequences following middle cerebral artery occlusion. J Cereb Blood Flow Metab. 1:53–60.

Tennant KA, Jones TA. 2009. Sensorimotor behavioral effects of endothelin-1 induced small cortical infarcts in C57BL/6 mice. J Neurosci Methods. 181:18–26.

Trachtenberg JT, Chen BE, Knott GW, Feng G, Sanes JR, Welker E, Svoboda K. 2002. Long-term in vivo imaging of experience-dependent synaptic plasticity in adult cortex. Nature. 420: 788–794.

Tuor UI, Wang R, Zhao Z, Foniok T, Rushforth D, Wamsteeker JI, Qiao M. 2007. Transient hypertension concurrent with forepaw stimulation enhances functional MRI responsiveness in infarct and peri-infarct regions. J Cereb Blood Flow Metab. 27:1819–1829.

Twitchell TE. 1951. The restoration of motor function following hemiplegia in man. Brain. 74:443–480.

Van der Gucht E, Hof PR, Van Brussel L, Burnat K, Arckens L. 2007. Neurofilament protein and neuronal activity markers define regional architectonic parcellation in the mouse visual cortex. Cereb Cortex. 17:2805–2819.

Ward NS. 2004. Functional reorganization of the cerebral motor system after stroke. Curr Opin Neurol. 17:725–730.

Watson BD, Dietrich WD, Busto R, Wachtel MS, Ginsberg MD. 1985. Induction of reproducible brain infarction by photochemically initiated thrombosis. Ann Neurol. 17:497–504.

Weber R, Ramos-Cabrer P, Justicia C, Wiedermann D, Strecker C, Sprenger C, Hoehn M. 2008. Early prediction of functional recovery after experimental stroke: functional magnetic resonance imaging, electrophysiology, and behavioral testing in rats. J Neurosci. 28:1022–1029.

Weiller C, Chollet F, Friston KJ, Wise RJ, Frackowiak RS. 1992. Functional reorganization of the brain in recovery from striatocapsular infarction in man. Ann Neurol. 31:463–472.

Wilbrecht L, Holtmaat A, Wright N, Fox K, Svoboda K. 2010. Structural plasticity underlies experience-dependent functional plasticity of cortical circuits. J Neurosci. 30:4927–4932.

Winship IR, Murphy TH. 2008. In vivo calcium imaging reveals functional rewiring of single somatosensory neurons after stroke. J Neurosci. 28:6592–6606.
Witte OW, Bidmon HJ, Schiene K, Redecker C, Hagemann G. 2000. Functional differentiation of multiple perilesional zones after focal cerebral ischemia. J Cereb Blood Flow Metab. 20:1149–1165.
Zhang ZG, Chopp M. 2009. Neurorestorative therapies for stroke: underlying mechanisms and translation to the clinic. Lancet Neurol. 8:491–500.
Zuo Y, Lin A, Chang P, Gan WB. 2005. Development of long-term dendritic spine stability in diverse regions of cerebral cortex. Neuron. 46:181–189.